Hydrogen/deuterium exchange behavior during denaturing/refolding processes determined in tetragonal hen egg-white lysozyme crystals

Akiko Kita* and Yukio Morimoto*

Institute for Integrated Radiation and Nuclear Science, Kyoto University, Kumatori, Sen-nan, Osaka 590-0494, Japan

*To whom correspondence should be addressed. Tel: +81-72-451-2379; Fax: +81-72-451-2635; E-mail: kita.akiko.4u@kyoto-u.ac.jp, and Tel/Fax: +81-72-451-2371; E-mail: morimoto.yukio.3z@kyoto-u.ac.jp

Keywords: hen egg-white lysozyme, H/D exchange, crystal structure, X/N joint refinement, denatured/refolded protein.

Synopsis

The crystal structure analyses of hen egg-white lysozymes containing traces of hydrogen/deuterium exchange during denaturing/refolding processes in solutions were performed using a joint X-ray and neutron refinement method. Differences in hydrogen/deuterium exchange were observed depending on the denaturing methods, acidic condition, basic condition, or thermal condition. This study describes the use of occupancy values determined by a crystallographic method for the analysis of protein denaturation.

Abstract

The hydrogen/deuterium (H/D) exchange of main chain amide hydrogens in the protein that denatured and refolded in deuterated solvent is considered to contain the traces of hydrogen bond cleavages or the exposure to solvent of the buried part of the protein during the denaturing/ and refolding (denaturing/refolding) processes. Here, we report the H/D exchange behaviors in hen egg-white lysozymes denatured under acidic conditions, basic conditions, and thermal conditions, and then refolded in deuterated solvents, using crystallographic methods. The results indicate that the space containing the Trp28 side chain was hardly exposed to the solvent in acidic conditions, but exposed under basic or heated conditions. Moreover, the β-bridges between Tyr53 and Ile58 in strands β2 and β3, which are in a highly conserved region, show some tolerance to changes in pD. The results indicate that crystallographic method is one of the powerful tools to analyze the denaturing/refolding processes of proteins.

1. Introduction

The elucidation of hydrogen/deuterium (H/D) exchange behavior is one of the methods to know fluctuations in the protein molecule [1]. Theoretically, dissociated hydrogen atoms, such as -NH_2, -SH, -OH, -COOH, and imide are exchangeable, whereas non-dissociated ones, such as -CH-, -CH2-, and -CH_3, are not. In general, dissociated hydrogen atoms buried in the protein core are not exchanged, whereas those exposed to the deuterated solvent are exchanged. Many H/D exchange studies of hen egg-white lysozyme (HWL) have been performed for the structural characterization, intermolecular interactions, or kinetics of denatured states [2-6]. For example, neutron diffraction methods had been applied to HWL crystals soaked in the deuterated ethanol solutions, in the deuterated dimethyl sulfoxide solutions, and in the deuterated tetramethylammonium chloride solutions, to know the binding mode of the small molecules, several decades ago [7-9].

Previously, we have reported an H/D substitution technique to increase H/D exchange via denaturing and refolding (denaturing/refolding) processes in deuterium solutions using HWL as a model protein [10]. HWL is an α/β protein consisting of an α-domain with a hydrophobic core and a β-strand domain [11]. When protein denaturation was achieved using acid, base, heat, and a combination of these methods, an increase in mass from the control protein that was prepared by dissolving HWL in

deuterium oxide (D_2O) was observed for each protein [10]. The increased H/D exchange positions in each denatured/refolded protein were considered to reflect the denatured positions in each process. As the increase in the mass of these denatured and refolded (denatured/refolded) proteins was not the same, the processes of denaturing these proteins were considered to be different.

To obtain information on the denaturing process that would be specific to each denaturing method, we have started the neutron diffraction studies of the control and denatured/refolded proteins. Neutron crystallography is a useful analysis method that not only determines the precise positions of hydrogen atoms, but also elucidates H/D exchange behaviors. Although the information about denaturing or folding processes are available by NMR studies [12], hydrogen-exchanged pulse-labelling mass-spectrometry method [13, 14], X-ray and neutron reflectometry [15], and so on, crystallographic methods are preferred for high molecular weight proteins. According to a previous report [2], only the backbone amide hydrogen atoms (hereinafter, abbreviated as main chain amide H or D) and the side chain indole NH hydrogen atoms of six Trps were considered for the examination of H/D exchange. We have reported the results of neutron diffraction studies for the control protein about the D occupancy [16], in which the H/D exchange effects (occupancies) of these atoms were categorized based on the previous reports [17-19]; deuterium atoms with occupancies refined to more than 0.7 were considered to be fully exchanged, whereas those refined to less than 0.15 were considered to be unexchanged. In addition to the previous baseline values of occupancies, in this report, we categorized Ds with occupancy values of 0.95-1.00 as "fully exchanged with the highest value", that of 0.6-0.69 as "quasi-exchanged", that of 0.16-0.25 as "quasi-unexchanged", and the other hydrogen atoms with their occupancies of 0.26-0.59 as "moderately exchanged", to understand the results of H/D exchange ratio values more easily (Figures 1 and 2). According to our categorization, the main chain amide Ds of Ala11, Asn19, Glu35, Thr47, Asp48, Asn59, Gly67, Asn74, Leu84, Asp101, Met105, Val109, Thr118, Gln121, and Leu129 were assigned as quasi-exchanged, those of Phe34, Asn39, Gln57, and Val99 were as quasi-unexchanged, and those of Leu8, Ala9, Asp18, Arg21, Ser24, Asn27, Val29, Thr51, Asn65, Arg68, Thr69, Ser86, Ala90, Lys97, Gly102, Gly104, Val120, and Arg125 were as moderately exchanged in the control structure (Figure 1a).

We compared the H/D exchange behaviors of the main chain amide Hs and the side chain indole NH hydrogen atoms of six Trps, between the control crystal structure and each denatured/refolded protein. The higher occupancy of deuterium atom than corresponding control atom indicates that the local disruption of hydrogen bonds or loosening of the structure have occurred. Therefore, H/D exchange behaviors contain the information about the denatured positions in each denaturing/refolding process.

2. Materials and methods

The model protein, HWL, was purchased and used (Sigma L6876-1G). As a standard protein solution of HWL, a 100% D_2O (Euriso-top, 99.9%) -solvated HWL solution at a concentration of 10 mg/mL was prepared and stored at 4˚C for at least 2 days. The protein was denatured by changing of the pD or by heating. To induce denaturation by a change in the pD, acidic conditions were prepared by the addition of deuterium chloride (DCl, 35 wt.% in D_2O, 99 atom % D, Sigma Aldrich), and basic conditions were prepared by the addition of sodium deuteroxide (NaOD, 30 wt.% in D_2O, 99 atom % D, Sigma Aldrich). Denatured proteins in both conditions were refolded by adjusting the $pH_{(read)}$ of each solution to around 7 by the addition of NaOD or DCl, respectively, after 1 day. To induce denaturation by heat, the protein solution was heated to 80˚C for 30 min. The details of the denaturing and refolding procedures are provided in the supplementary materials. Finally, all protein solutions were concentrated to more than approximately 100 mg/mL and stored at 4 C˚ until use.

Crystallization, and neutron and X-ray data collections for denatured/refolded proteins were performed in accordance with those of control protein [16]. The solutions of 3% - 4% sodium chloride in deuterated 0.1 M sodium acetate ($pH_{(read)}$ 4.6) were prepared and used for crystallization solutions. The sitting-drop vapor diffusion method, in which filtered drop solutions (4μl) containing protein and the same volume of crystallization solutions were equilibrated against the crystallization solutions, was employed. Only one or two crystals were appeared in each batch at 20˚C after more than 1-2 weeks with high probability. The crystals for neutron diffraction studies were grown by the repeated addition of protein solutions that contained deuterated precipitant reagents to each batch in which only one crystal was appeared. The crystals used for neutron diffraction studies are shown in Figure S1. The crystals for X-ray diffraction studies were obtained under the same conditions as for neutron data collection.

Neutron data were collected at room temperature using a Laue diffractometer CG-4D's IMAGINE installed at the High Flux Isotope Reactor at Oak Ridge National Laboratory [20, 21]. The X-ray data were collected at room temperature using CuKα radiation from a rotating anode X-ray source with a RAXIS VII imaging plate detector (Rigaku).

The X-ray structures were solved by the molecular replacement method using the coordinates of H/D exchanged lysozyme (wwPDB Code: 6K8G.pdb) [16]. The X/N joint refinement was carried out using X-ray and neutron data with the PHENIX software package [22]. The quality of the model was checked using the MolProbity server at http://molprobity.biochem.duke.edu/ [23]. Pictures were prepared using the program PyMOL Molecular Graphic System program (Version 1.2r3pre, Schrodinger, LLC). The details of experiments, and data collection and the refinement statistics are summarized in the supplementary materials and Table 1.

3. Results

3.1. Overall structure of HWL

The X-ray crystal structure analyses of deuterated HWLs denatured under different conditions were performed 2Å resolution. Three denaturing conditions were used: acidic conditions (below $pH_{(read)}$ 2.0), produced by the addition of DCl and refolded by the addition of NaOD solutions (abbreviated as DLysCl); basic conditions (over $pH_{(read)}$ 11.0), produced by the addition of NaOD and refolded by the addition of DCl solutions (abbreviated as DLysOD); and heat conditions (80 ˚C for 30 min.), and refolded by cooling to R.T. (abbreviated as DLyshc). The structures of the refolded proteins were similar to that of control (PDB code: 6K8G) [16]. The neutron crystal structure analyses were carried out at 2Å resolution (DLysCl and DLyshc) and 2.3Å resolution (DLysOD). The differences in the resolution of neutron diffraction data would arise from the crystal size; the volume of the DLysOD crystal was smaller than the others. The crystals and neutron density map for each denatured/refolded protein are shown in Figures S1 and S2.

The occupancy values for main chain amide Ds for the control and denatured/refolded proteins are plotted against the amino acid residue number (Figures 1a, b, d, and f). The difference in the occupancy values for main chain amide Ds between the control [16] and each sample was also plotted (Figures 1c, e, and g). The

result of the increased mass values calculated from the occupancy values of all atoms of DLysCl, DLysOD, and DLyshc shows that DLysOD is the highest among these samples. This is consistent with our previous results [10]. The overall structure for each sample is drawn in Figure S3. The deuterium atoms with an occupancy value extremely lower than the corresponding control D are excluded further in this report, as they are unlikely in the experimental system. The main chain amide Ds and Ds at the side chains of Trps excluded due to the unlikely occupancy values are colored in gray in each figure, unless otherwise stated.

3.2. Lysozyme denatured in acidic condition and refolded in D_2O (DLysCl)

The occupancy values for main chain amide Ds of the control [16] and DLysCl, and the differences between them, are shown in Figures 1(a) - (c). The regions in which an obvious increase of occupancy values for several main chain amide Ds were observed are the first half of helix1 (Leu8-Lys13), both ends of helix 3 (Asn27 and Phe34), and the buried part of helix 5 (Leu83). (Figures 2a, and S3) In addition, the increasements of the deuterium occupancies in the loop region, at Phe38 and Asn39, which follow part of the helix 3 and form hydrogen bonds with Ser36, respectively, were observed. The side chains of Trp62, Trp63, Trp108, and Trp111 were fully exchanged, that of Trp123 was quasi-exchanged, and that of Trp28 was quasi-unexchanged.

Conversely, the residues whose main chain amide Hs were unexchanged or quasi-unexchanged to Ds are Met12 in helix1, Trp28 - Lys33 in helix 3, Tyr53, Gln57 and Ile58 in β-sheet, and Val92, Ala95, and Lys96 in helix 6. (Figures 2a, and S3) Many of these residues are related to form the hydrophobic core of α-domain; e.g., the residues Met12, Trp28, and Val92 are the members of the hydrophobic core cluster, and Gln57, Ile58, and Lys96 are close to hydrophobic core members. These results indicate that the hydrophobic core of the α-domain are relatively unaffected by the acidic conditions. This is consistent with the fact that the side chain D of Trp28, which is buried in the α-domain, has a low occupancy value in DLysCl. (Figure 2a)

3.3. Lysozyme denatured in basic condition and refolded in D_2O (DLysOD)

The occupancy values for the main chain amide Ds of DLysOD, and the differences between the control and DLysOD, are shown in Figures 1(d) and 1(e). From the comparison of the deuterium occupancy values of main chain amides with those of

control, the atoms with a clear increase from the control are contained in helices 1, 3, 4, 5, and 6, and β-strands 2 and 3. (Figures 1d, e, and S3) During the denaturing/refolding process, almost all of the hydrogen bonds which are contained in helices 1, 4, and 5 appear to be disrupted.

On the contrary, a few main chain amide Hs in DLysOD are unexchanged; the main chain amide H of Tyr53 in strand 2 was unexchanged, and those of Arg21 and Thr47 in the loop region, Trp28 - Cys30 in helix 3, Ile58 in strand 3, and Ala95 in helix 6 were not exchanged to some extent. Among these, two residues, Tyr53 and Ile58 are β-bridge partners in the β-sheet. These H/D exchange observations suggest that hydrogen bonds between Tyr53 and Ile58 were hardly broken, and that those in helix 3 were not completely disrupted during the denaturing process in the basic conditions (Figure 2b). Moreover, the side chains of Trps28, Trp108, Trp111, and Trp123 are in the fully exchanged category. The result that the side chain NH atom of Trp28, which was not exchanged in control protein [16], is fully exchanged to D means that the core of the α-domain was exposed to the outer solution during the denaturing/refolding processes (Figure 2a).

3.4. Lysozyme denatured at 80°C and refolded by cooling (DLyshc)

The occupancies of main chain amide Ds of DLyshc, and the differences of H/D exchange behaviors from those of control are shown in Figure 1(f) and 1(g). In DLyshc, most of the main chain amide Ds are categorized in fully- and quasi-exchanged. The increasement of occupancy values of main chain amide Ds compared with those of the control were observed in helices 1, 3, 4, 5, and 6, and β-strands 2 and 3. The main chain amide Hs in these helices are almost all categorized as fully exchanged, even those that face inside of the α-domain core. These results are consistent with the observation of the Trp28 side chain, which was fully exchanged in DLyshc. As for the side chains of other Trps, the side chains of Trp108, Trp111, and Trp123 were fully exchanged, and that of Trp62 and Trp63 were moderately exchanged.

4. Discussion

In a previous report [6], H/D exchange kinetics in the acidic conditions were studied for the HWL sample in which the Cys6-Cys127 disulfide bond was selectively cleaved. In that, it was suggested that H/D exchanges in the main chain amide Hs of Ala10,

Met12, and Lys13, which are in the latter half of helix 1, were too fast to be accurately measured. In contrast, in DLysCl in our study, main chain amide H of Met12 was quasi-unexchanged, and that of Ala10 was moderately exchanged. These results suggest that disulfide bonds would contribute to the stability of hydrogen bonds in helices. Considering this, other disulfide bonds would also affect the H/D exchange behaviors; e.g., in the helices 3 and 6, which are longer than helix 1, the hydrogen-remained parts are located at the central part of the helices, which contain disulfide bonds (Cys30-Cys115 and Cys94-Cys76). However, the relative positions of the hydrogen-remained residues to the disulfide bond in helices 3~~,~~ and 6 are not agree with that of helix 1; the hydrogens in close proximity the cysteine residues remained in helices 3 and 6, and the hydrogen-bonded partner of cysteine or H in residues further away in the helical structure remained in helix 1. Therefore, it could not be determined whether the stability of hydrogen bonds in the central region in helices 3 and 6 is due to the disulfide bonds, the properties of the long helix, or both.

We focused on the H/D exchange behavior of the side chain of Trp28, which is located in the buried space of α-domain and surrounded with helices 1, 2, 3, 6, and 7, and the loop between β strands 2 and 3. Our results indicate that the Trp28 side chain was not exposed to the solvent in control and acidic conditions, however, it was exposed to the solvent in basic and heat conditions. These results are consistent with reports that HWL is not induced to the molten globule (MG) state at very low pH [24] but at alkali conditions [25], and that unfolding of nearly 50% of the helical structure occurs at a temperature higher than 70 ˚C [26]. The control, DLysCl, and DLysOD have common H/D exchange tendencies in helices of 1, 3, and 6, in which the residues in the central part are unexchanged, to some extent (Figure 2a). Therefore, the differences in H/D exchange behaviors of Trp28 between the control and DLysCL, and DLysOD would come from the degree of disruption of the hydrogen bonds included in the elements of α-domain core. Besides in DLyshc, the main chain amides with especially high occupancy with the highest value (0.95-1) were observed at the residues that faced the inside of the α-domain core and were located in the central part of the helices 3 and 6, and helix 1 (Figure 2a). This means that the process of thermal denaturation in HWL may be different from that caused by a change in pD.

In the lysozyme superfamily and subfamilies (GH19, GH22, G23, GH24, and GH46), the β-hairpin structure, which points toward the substrate binding cleft and

contains a catalytic residue, is one of two common structural elements defined in the signature motif, and show the highest amino acid conservation in sequences alignment [27]. In HWL, β-strands 2 and 3 forms the β-hairpin structure corresponding to this signature motif. It is notable that the hydrogen bonds between Tyr53 in β-strand 2 and Ile58 in β-strand 3 showed tolerance to H/D exchange in denaturation caused changes in pD. In addition, the residues Tyr53 and Ile58 are among the residues with main chain amide exchange rates significantly slower than predicted in acid-denatured CM^{6-127} lysozyme [6]. These results indicate that there may be a relationship between the stability of hydrogen bonds and the functionally conserved structures and amino acids.

There are many unknowns in the field of H/D exchange of protein, for examples, the relationship between H/D exchange and the distance from surface [28]. However, it is possible to obtain information about denaturing events by comparing the H/D exchange observations between the control and denatured/refolded protein, and some techniques, for example, H/D exchange mass spectrometry method [29] or NMR method [30], have been used. In addition to these methods, we reported here that it is also possible to know the trace aspects of the denaturing/refolding processes, such as hydrogen bond disruption, by a crystallographic method. Despite crystallographic methods are not appropriate for some proteins which are difficult to crystallize, or such as intrinsically disordered proteins which lack stable tertiary structure, crystallography is one of a powerful tools to obtain information about structure with no size limitation, theoretically. To identify some rules related to breaking hydrogen bonds during denaturing/refolding processes, more information is required about H/D exchange observations for many different types of protein molecules, especially those with a high molecular weight, with sufficiently high resolution data to refine the occupancy values of the exchangeable deuterium atoms. This is one of the useful techniques to know the intrinsic properties of the protein structures and to examine molecular evolution.

Accession number

The structure factors and coordinates have been deposited in the Worldwide Protein Data Bank under accession numbers 7FG8, 7FGU, and 7FGV for DLysCl, DLysOD, and DLyshc, respectively.

Acknowledgements

We thank Dr. Andrey Kovalevsky and the staff members at the beamlines of IMAGINE, HFIR at the ORNL under the proposals IPTS-18574.1, 19637.1, 19782.1, and 20561.1; and Dr. Alison Edwards and Dr. Ross Piltz for the KOALA, OPAL at the ANSTO under proposal P6087, for their help with neutron data collection; and Prof. Kunio Miki and his group at the Graduate School of Science, Kyoto University, for their kind help with X-ray data collection, biochemical experiments, and fruitful discussion.

Funding information

This work was supported by the Photon and Quantum Basic Research Coordinated Development Program from the Ministry of Education, Culture, Sports, Science and Technology, Japan (2013-2017 to A. K. and Y. M.); by the Research Development Program “Ishizue” of Kyoto University (2017 to A.K.); by the Future Development Funding Program of Kyoto University Research Coordination Alliance (2018 to A.K.); by The Towa Foundation for Food Science & Research (2018 to A.K.); and by The Kyoto University Foundation (2020 to A. K.).

Conflict of interest

There are no known conflicts of interest associated with this publication and there has been no significant financial support for this work that could have influenced its outcome.

References

1. Kossiakoff, A. A. (1982) Protein dynamics investigated by the neutron diffraction–hydrogen exchange technique. Nature 296, 713-721. DOI: 10.1038/296713a0
2. Bentley, G. A., Delepierre, M., Dobson, C. M., Wedin, R. E., Mason, S. A. and Poulsen, F. M. (1983) Exchange of individual hydrogens for a protein in a crystal and in solution. J. Mol. Biol. 170, 243-247. DOI: 10.1016/s0022-2836(83)80235-6
3. Mason, S. A., Bentley, G. A. and McIntyre, G. J. (1984) Deuterium exchange in lysozyme at 1.4-A resolution. Basic Life. Sci. 27, 323-334. DOI: 10.1007/978-1-4899-0375-4_19

4. Delepierre, M., Dobson, C. M., Karplus, M., Poulsen, F. M., States, D. J. and Wedin, R. E. (1987) Electrostatic effects and hydrogen exchange behaviour in proteins. The pH dependence of exchange rates in lysozyme. J. Mol. Biol. 197, 111-130. DOI: 10.1016/0022-2836(87)90613-9
5. Pedersen, T. G., Sigurskjold, B. W., Andersen, K. V., Kjaer, M., Poulsen, F. M., Dobson, C. M. and Redfield, C. (1991) A nuclear magnetic resonance study of the hydrogen-exchange behaviour of lysozyme in crystals and solution. J. Mol. Biol. 218, 413-426. DOI: 10.1016/0022-2836(91)90722-i
6. Radford, S. E., Buck, M., Topping, K. D., Dobson, C. M. and Evans, P. A. (1992) Hydrogen exchange in native and denatured states of hen egg-white lysozyme. Proteins 14, 237-248. DOI: 10.1002/prot.340140210
7. Lehmann, M. S., Mason, S. A., and McIntyre, G. J. (1985) Study of ethanol-lysozyme interactions using neutron diffraction. Biochemistry 24, 5862-5869. DOI: 10.1021/bi00342a026
8. Lehmann, M. S. and Stansfield, R. F. (1989) Binding of dimethyl sulfoxide to lysozyme in crystals, studied with neutron diffraction. Biochemistry 28, 7028-7033. DOI: 10.1021/bi00443a037
9. Bouquiere, J. P., Finney, J. L., and Lehmann, M. S. (1993) Interaction of the tetramethylammonium ion with the lysozyme molecule, studied using neutron diffraction. *J. Chem. Soc. Faraday Trans.* 89, 2701-2705. DOI: 10.1039/FT9938902701
10. Kita, A. and Morimoto, Y. (2016) An effective deuterium exchange method for neutron crystal structure analysis with unfolding–refolding processes. Mol. Biotechnol. 58, 130-136. DOI: 10.1007/s12033-015-9908-8
11. Blake, C. C. F., Koenig, D. F., Mair G. A., North, A. C. T., Phillips, D. C. and Sarma, V. R. (1965) Structure of hen egg-white lysozyme: a three-dimensional fourier synthesis at 2 Å resolution. Nature 206, 757-761. DOI: 10.1038/206757a0
12. Baum, J., Dobson, C. M., Evans, P. A., and Hanley, C. (1989) Characterization of a partly folded protein by NMR methods: studies on the molten globule state of guinea pig alpha-lactoalbumin. Biochemistry 28, 7-13. DOI: 10.1021/bi00427a002
13. Walters, B. T., Mayne, L., Hinshaw, J. R., Sosnick, T. R., and Englander, S. W. (2013) Folding of a large protein at high structural resolution. Proc. Natl. Acad. Sci. U. S. A. 110, 18898-18903. DOI: 10.1073/pnas.1319482110

14. Georgescauld, F., Popova, K., Gupta, A. J., Bracher, A., Engen, J. R., Hayer-Hartle, M., and Hartl, F. U. (2014) GroEL/ES chaperonin modulates the mechanism and accelerates the rate of TIM-barrel domain folding. Cell 157, 922-934. DOI: 10.1016/j.cell.2014.03.038
15. Akgun, B., Satija, S., Nanda, H., Pirrone, G. F., Shi, X., Engen, J. R. and Kent, M. S. (2013) Conformational transition of membrane-associated terminally acylated HIV-1 Nef. Structure 21, 1822-1833. DOI: 10.1016/j.str.2013.08.008
16. Kita, A. and Morimoto, Y. (2020) Hydrogen/deuterium exchange behavior in tetragonal hen egg-white lysozyme crystals affected by solution state. J. Appl. Crystallogr. 53, 837-840. DOI: 10.1107/S1600576720005488
17. Bennett, B., Langan, P., Coates, L., Mustyakimov, M., Schoenborn, B., Howell, E. E. and Dealwis, C. (2006) Neutron diffraction studies of Escherichia coli dihydrofolate reductase complexed with methotrexate. Proc. Natl. Acad. Sci. U. S. A. 103,18493-18498. DOI: 10.1073/pnas.0604977103
18. Sukumar, N., Mathews, F. S., Langan, P. and Davidson, V. L. (2010) A joint x-ray and neutron study on amicyanin reveals the role of protein dynamics in electron transfer. Proc. Natl. Acad. Sci. U. S. A. 107, 6817-6822. DOI: 10.1073/pnas.0912672107
19. Wan, Q., Bennett, B. C., Wilson, M. A., Kovalevsky, A., Langan, P., Howell, E. E. and Dealwis, C. (2014) Toward resolving the catalytic mechanism of dihydrofolate reductase using neutron and ultrahigh-resolution X-ray crystallography. Proc. Natl. Acad. Sci. U. S. A. 111, 18225-18230. DOI: 10.1073/pnas.1415856111
20. Meilleur, F., Munshi, P., Robertson, L., Stoica, A. D., Crow, L., Kovalevsky, A., Koritsanszky, T., Chakoumakos, B. C., Blessing, R. and Myles, D. A. A. (2013) The IMAGINE instrument: first neutron protein structure and new capabilities for neutron macromolecular crystallography. Acta Crystallogr. D69, 2157-2160. DOI: 10.1107/S0907444913019604
21. Schröder, G. C., O'Dell, W. B., Myles, D. A. A., Kovalevsky, A. and Meilleur, F. (2018) IMAGINE: neutrons reveal enzyme chemistry. Acta Crystallogr. D74, 778-786. DOI: 10.1107/S2059798318001626
22. Liebschner, D., Afonine, P. V., Baker, M. L., Bunkoczi, G., Chen, V. B., Croll, T. I., Hintze, B., Hung, L.-W., Jain, S., McCoy, A. J., Moriarty, N. W., Oeffner, R. D., Poon, B. K., Prisant, M. G., Read, R. J., Richardson, J. S., Richardson, D. C.,

Sammito, M. D., Sobolev, O. V., Stockwell, D. H., Terwilliger, T. C., Urzhumtsev, A. G., Videau, L. L., Williams, C. J. and Adams, P. D. (2019) Macromolecular structure determination using X-rays, neutrons and electrons: recent developments in Phenix. Acta Crystallogr. D75, 861-877. DOI: 10.1107/S2059798319011471

23. Williams, C, J., Headd, J. J., Moriarty, N. W., Prisant, M. G., Videau, L. L., Deis, L. N., Verma, V., Keedy, D. A., Hintze, B. J., Chen, V. B., Jain, S., Lewis, S. M., Arendall 3rd, W. B., Snoeyink, J., Adams, P. D., Lovell, S. C., Richardson, J. S. and Richardson, D. C. (2018) MolProbity: More and better reference data for improved all-atom structure validation. Protein Sci. 27, 293-315. DOI: 10.1002/pro.3330

24. Fink, A. L., Calciano, L. J., Goto, Y., Kurotsu, T., and Palleros, D. R. (1994) Classification of acid denaturation of proteins: intermediates and unfolded states. Biochemistry 33, 12504-12511. DOI: 10.1021/bi00207a018

25. Hameed, M., Ahmad, B., Fazili, K. M., Andrabi, K. and Khan, R. H. (2007) Different molten globule-like folding intermediates of hen egg white lysozyme induced by high pH and tertiary butanol. J. Biochem. 141, 573-583. DOI: 10.1093/jb/mvm057

26. Meersman, F., Atilgan, C., Miles, A. J., Bader, R., Shang, W., Matagne, A., Wallace, B. A., and Koch, M. H. J. (2010) Consistent picture of reversible thermal unfolding of hen egg-white lysozyme from experiment and molecular dynamics. Biophys. J. 99, 2255-2263. DOI: 10.1016/j.bpj.2010.07.060

27. Wohlkonig, A., Huet, J., Looze, Y. and Wintjens, R. (2010) Structural relationships in the lysozyme superfamily: significant evidence for glycoside hydrolase signature motifs. Plos One 5, e15388. DOI: 10.1371/journal.pone.0015388

28. McAllister, R. G. and Konermann, L. (2015) Challenges in the interpretation of protein H/D exchange data: a molecular dynamics simulation perspective. Biochemistry 54, 2683-2692. DOI: 10.1021/acs.biochem.5b00215

29. James, E. I., Murphree, T. A., Vorauer, C., Engen, J. R. and Guttman, M. (2021) Advances in hydrogen/deuterium exchange mass spectrometry and the pursuit of challenging biological systems. Chem. Rev. *in pres*s DOI: 10.1021/acs.chemrev.1c00279

30. Krishna, M. M. G., Hoang, L., Lin, Y. and Englander, S. W. (2004) Hydrogen exchange methods to study protein folding. Methods. 34, 51-64. DOI: 10.1016/j.ymeth.2004.03.005

31. Oostenbrink, C., Soares, T. A., van der Vegt, N. F. A. and van Gunsteren W. F. (2005) Validation of the 53A6 GROMOS force field. Euro. Biophys. J. 34, 273-284. DOI: 10.1007/s00249-004-0448-6

Figure legends

Figure 1.

The H/D exchange behavior of main chain amide hydrogen atoms of control and denatured/refolded proteins. The main chain amide deuterium occupancies were plotted versus residue number. Colors on the graphs indicate the categories of deuterium occupancy; the occupancy values above 0.95: magenta; 0.7-0.94: orange, 0.6-0.69: yellow; 0.26-0.59: white; 0.16-0.25 : green; and below 0.15: cyan. The difference between the control and each denatured/refolded protein was also plotted. The secondary structures are drawn over the graph [31]. (a), (b), (d), and (f): The occupancy values of main chain amide Ds of the control, DLysCl, DLysOD, and DLyshc structures. (c), (e), and (g): The difference in the occupancy value of each main chain amide D between the control and DLysCl (DLysCl-control), DLysOD (DLysOD-control), and DLyshc (DLyshc-control).

Figure 2.

The H/D exchange behaviors of the control and denatured/refolded proteins. The colors are same as Figure 1; the occupancy values above 0.95: magenta; 0.7-0.94 : orange, 0.6-0.69: yellow; 0.26-0.59: white; 0.16-0.25: green; and below 0.15: cyan. Helix 2 (Tyr20-Gly22) is depicted by a loop model for easy observation. (a) The hydrophobic core of the α-domain in the control and each denatured/refolded protein. The side chains of Trp28s and disulfide bonds were also drawn. (b) The hydrogen bonds between Tyr53 in S2 and Ile58 in S3.

Hydrogen/deuterium exchange behavior during denaturing/refolding processes determined in tetragonal hen egg-white lysozyme crystals

Abstract

This supplementary material provides the following information;

1. Sample preparation and crystallization

2. Neutron and X-ray diffraction experiments

3. Quality of neutron density map

4. Figure legend

1. Sample preparation and crystallization

Hen egg-white lysozyme was purchased (HWL, Sigma L6876-1G). As a standard protein solution, a 100% D_2O (Euriso-top, 99.9%) -solvated HWL solution at a concentration of 10 mg/mL was prepared and stored at 4˚C for at least 2 days. For the pD-induced denaturation of the proteins, DCl (35 wt. % in D_2O, 99 atom % D, Sigma Aldrich) or NaOD (30 wt. % in D_2O, 99 atom % D, Sigma Aldrich) was added at a 1:1000 volumetric ratio to the HWL solution. The $pH_{(read)}$ of the DCl-added HWL solution was less than 2, and that of the NaOD-added HWL solution was over 11. Denatured solutions were stored at 4˚C for 1 day. The refolding of pD-induced denatured proteins was done by returning the $pH_{(read)}$ to around 7 using NaOD or DCl. The $pH_{(read)}$ value of the protein solution was measured using a compact pH meter (HORIBA compact pH meter twin B-212). After denaturing/refolding processes by a change in pD, the refolded protein solutions that contained NaOD and DCl were replaced with D_2O by repeated ultrafiltration/dilution procedures with viva spin series (Sartorius) and Amicon Ultra series (Merck Milipore), to reduce the concentration of the solutions to less than 1/1000 of the initial value. For thermal denaturation of the protein, heat treatment of HWL at 10mg /mL was performed at 80˚C for 30 min. After heat treatment, the protein sample was cooled at R.T. and therefore, incubated at 4˚C at least overnight. All protein solutions were concentrated to 100 mg/mL and stored at 4˚C until use. Crystallization solutions of 3% - 4% sodium chloride in 0.1 M sodium acetate ($pH_{(read)}$ 4.6) prepared with sodium acetate-d_3 (Sigma Aldrich, 99 atom % D), acetic acid-d_4 (Sigma Aldrich, 99.5 atom % D), and 100% D_2O, were used. The sitting-drop vapor diffusion technique was used for crystallization. The drop solutions, which are the mixtures of protein solution and the same volume of crystallization solutions, were filtered using a 0.1 μm filter (Ultrafree-MC Centrifugal Filter UFC30VV00, Merck Millipore) to suppress excessive nucleation. Droplets (4 μl) of the drop solutions were placed on the Fluorinert liquid (Hampton Research) on the sitting drop well to prevent the crystals from sticking to the surface of the crystallization plate, and equilibrated against crystallization solutions. Only one or two crystals were appeared in each batch at room temperature (20˚C) after more than 1-2 weeks with high probability. The crystals were grown by addition of a mixture solutions of stock protein containing crystallization solution. After more than 3 months and after more than 15 times additions of mixture solution, crystals large

enough for the neutron diffraction work were obtained (Figure S1).

2. Neutron and X-ray diffraction experiments

The crystals for neutron diffraction were mounted in quartz capillaries with a trace amount of mother liquor, and the neutron data were collected at room temperature with Laue diffractometer CG-4D's IMAGINE installed at the High Flux Isotope Reactor at Oak Ridge National Laboratory [1-2]. The neutron quasi-Laue single crystal diffraction intensities were collected with an exposure time of 20 h (DLysCl and DLyshc) or 18-20 h (DLysOD) per each frame. The data were processed using LAUEGEN, and the data were normalized and merged using the LSCALE and SCALA programs [3-7]. The X-ray data were collected using the crystals obtained in the same crystallization conditions used for neutron data collection. The crystals were mounted in soda-glass capillaries, and the X-ray data were collected at room temperature using CuKα radiation from a rotating anode X-ray source with an RAXIS VII imaging plate detector (Rigaku). The oscillation range was 1.0˚ and the exposure time was 1 min. per image. Diffraction data were processed with the HKL2000 package [8]. The X-ray structure was solved by the molecular replacement method using the coordinates of H/D exchanged lysozyme (PDB code: 6K8G.pdb [9]). The coordinates for H/D exchanged HWL were initially refined against X-ray data. After the R-factors converged, the X/N joint refinement was carried out using X-ray and neutron data with PHENIX software package [10]. Deuterium atoms at the N-terminus (Lys1) were added manually. Manual model building during the refinement procedures was carried out using COOT [11].

3. Quality of neutron density map

The 2Fo-Fc nuclear density maps clearly showed that each hydrogen atom bound to Nε1 of Trp28 in DLysOD and DLyshc, was exchanged to deuterium. The occupancies of these deuterium atoms were 1.00 and 0.98, respectively. However, the occupancy of deuterium atom bond to Nε1 of Trp28 in DLysCl was very low, with the calculated value of 0.19. The neutron density maps of these residues are shown in Figure S2. Pictures for structures were prepared using the program PyMOL Molecular Graphic System program (Version 1.2r3pre, Schrodinger, LLC).

4. Figure legends.

Figure S1.

The crystals of denatured/refolded HWL used for neutron diffraction experiments in this study. (a) DLysCl, (b) DLysOD, and (c) DLyshc.

Figure S2.

X-ray and neutron density maps calculated using the each model protein without D/H that binds to Trp28Nε1. The 2Fo-Fc X-ray density map (blue, 1.2 σ), the 2Fo-Fc neutron-scattering length density map (green, 1.2 σ), and the Fo-Fc neutron-scattering length density map (red, 3.0 σ) are drawn. The colors of protein residues are same as Figures 1 and 2.

Figure S3.

The overall structures of control, DLysCl, DLysOD, and DLyshc. The colors on main chain ribbon models are same as Figures 1 and 2, and two proline residues (Pro70 and Pro79) are colored in dark gray. The side chain of the six Trps and the disulfide bonds are drawn as stick models to show their location.

References

1. Meilleur, F., Munshi, P., Robertson, L., Stoica, A. D., Crow, L., Kovalevsky, A., Koritsanszky, T., Chakoumakos, B. C., Blessing, R. and Myles, D. A. A. (2013) The IMAGINE instrument: first neutron protein structure and new capabilities for neutron macromolecular crystallography. Acta Crystallogr. D69, 2157-2160. DOI: 10.1107/S0907444913019604
2. Schröder, G. C., O'Dell, W. B., Myles, D. A. A., Kovalevsky, A. and Meilleur, F. (2018) IMAGINE: neutrons reveal enzyme chemistry. Acta Crystallogr. D74, 778-786. DOI: 10.1107/S2059798318001626
3. Helliwell, J. R., Habash, J., Cruickshank, D. W. J., Harding, M. M., Greenhough, T. J., Campbell, J. W., Clifton, I. J., Elder, M., Machin, P. A., Papiz, M. Z. and Zurek, S. (1989) The recording and analysis of synchrotron X-radiation Laue diffraction photographs. J. Appl. Crystallogr. 22, 483-497. DOI: 10.1107/S0021889889006564

4. Campbell, J. W. (1995) LAUEGEN, an X-windows-based program for the processing of Laue diffraction data. J. Appl. Crystallogr 28, 228-236. DOI: 10.1107/S002188989400991X

5. Campbell, J. W., Hao, Q., Harding, M. M., Nguti, N. D. and Wilkinson, C. (1998) LAUEGEN version 6.0 and INTLDM. J. Appl. Crystallogr. 31, 496-502. DOI: 10.1107/S0021889897016683
6. Arzt, S., Campbell, J. W., Harding, M. M., Hao, Q. and Helliwell, J. R. (1999) LSCALE– the new normalization, scaling and absorption correction program in the Daresbury Laue software suite. J. Appl. Crystallogr. 32, 554-562. DOI: 10.1107/S0021889898015350
7. Weiss, M. S. (2001) Global indicators of X-ray data quality. J. Appl. Crystallogr. 34, 130-135. DOI: 10.1107/S0021889800018227
8. Otwinowski, Z. and Minor, W. (1997) Processing of X-ray diffraction data collected in oscillation mode. Methods Enzymol. 276, 307-326.
9. Kita, A. and Morimoto, Y. (2020) Hydrogen/deuterium exchange behavior in tetragonal hen egg-white lysozyme crystals affected by solution state. J. Appl. Crystallogr. 53, 837-840. DOI: 10.1107/S1600576720005488
10. Liebschner, D., Afonine, P. V., Baker, M. L., Bunkoczi, G., Chen, V. B., Croll, T. I., Hintze, B., Hung, L.-W., Jain, S., McCoy, A. J., Moriarty, N. W., Oeffner, R. D., Poon, B. K., Prisant, M. G., Read, R. J., Richardson, J. S., Richardson, D. C., Sammito, M. D., Sobolev, O. V., Stockwell, D. H., Terwilliger, T. C., Urzhumtsev, A. G., Videau, L. L., Williams, C. J. and Adams, P. D. (2019) Macromolecular structure determination using X-rays, neutrons and electrons: recent developments in Phenix. Acta Crystallogr. D75, 861-877. DOI: 10.1107/S2059798319011471
11. Emsley, P. and Cowtan, K. (2004) Coot: model-building tools for molecular graphics. Acta Crystallogr. D60, 2126-2132. DOI: 10.1107/S0907444904019158

Table I. data statistics and refinement parameters

Molecule	DLysCl		DLysOD		DLyshc	
PDB code	7FG8		7FGU		7FGV	
Data collection	Xray	Neutron	Xray	Neutron	Xray	Neutron
Wavelength (Å)	1.54	2.8-4.5	1.54	2.8-4.5	1.54	2.8-4.5
No. frames	100	15	93	13	100	9
Resolution (Å)	2.0	1.998	2.0	2.3	2.0	2.0
(Outer shell)	(2.07-2.00)	(2.11-2.00)	(2.07-2.00)	(2.42-2.29)	(2.07-2.00)	(2.11-2.00)
Measurements	124,136	64,209	115,426	33,224	115,902	38,648
Unique reflections	8,580	7,546	8,548	4,857	8,521	7,100
R_{merge}[a]	0.027 (0.080)	0.166 (0.268)	0.032 (0.098)	0.156 (0.285)	0.055 (0.139)	0.169 (0.268)
Redundancy	14.5 (10.2)	8.5 (7.0)	13.5 (10.0)	6.8 (6.3)	13.6 (9.2)	5.4 (4.4)
Completeness (%)	99.6 (96.4)	91.0 (84.6)	99.2 (92.2)	87.7 (76.0)	98.7 (91.8)	86.4 (78.9)
I/s (I)	67.6 (26.5)	6.5 (4.1)	64.0 (23.6)	6.0 (4.0)	42.1 (11.9)	5.0 (3.2)
Refinement						
Space group	$P4_32_12$		$P4_32_12$		$P4_32_12$	
Cell dimensions (Å)						
a	79.2		79.3		79.2	
c	37.9		37.9		37.9	
R_{work}/R_{free}[b,c] (%)	0.140/0.183	0.233/0.266	0.132/0.171	0.220/0.266	0.141/0.182	0.224/0.250
No. of non-H/D atoms						
Protein	997		997		997	
Others (solvent, Na, Cl)	88		86		88	
No. of deuterium atoms						
Protein	261		260		262	
Solvent	130		98		128	
Average B factors (Å^2)						
Non-H/D atoms protein/ others	21.5/32.6		22.4/32.9		21.2/32.8	
Deuterium atoms protein/ others	32.2/38.0		32.6/37.0		31.7/37.9	
Rmsd bond length (Å)	0.006		0.006		0.006	
Rmsd bond angles (deg.)	0.817		0.875		0.835	

[a] $R_{merge} = \Sigma\ (|I-\langle I\rangle|)/\Sigma\ (I)$

[b] $R = \Sigma||F_{obs}|-|F_{calc}||/\ \Sigma|F_{obs}|$

[c] R_{work} is calculated from a set of reflections in which 5% of the total reflections have been randomly omitted from the refinement and used to calculate R_{free}.

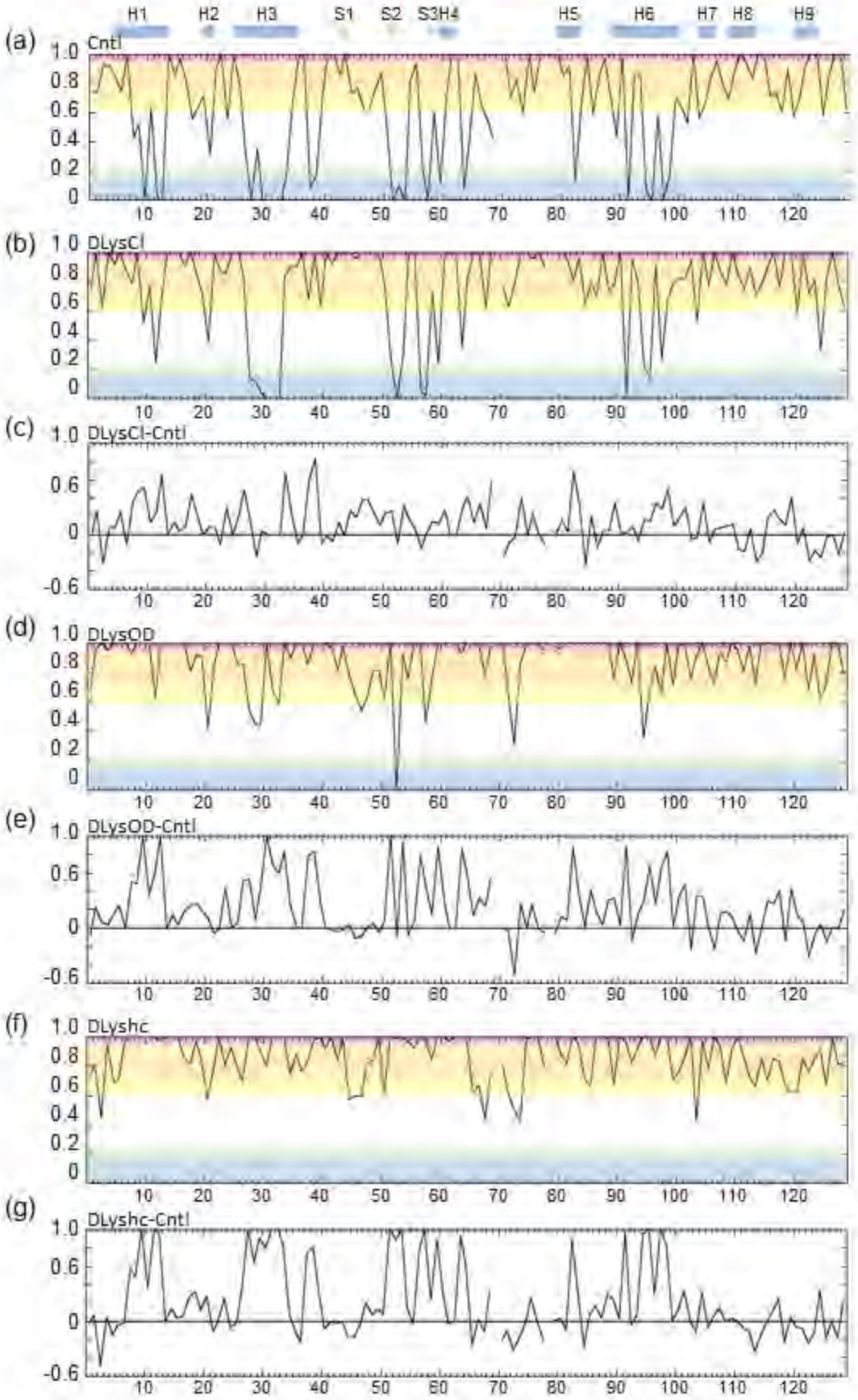
H1
H2
H3
S1
S2
S3H4
H5
H6
H7
H8
H9
(a)
Cntl
(b)
DLysCl
(c)
DLysCl-Cntl
(d)
DLysOD
(e)
DLysOD-Cntl
(f)
DLyshc
(g)
DLyshc-Cntl
1.0
0.8
0.6
0.4
0.2
0
-0.6
10
20
30
40
50
60
70
80
90
100
110
120

Figure 1

(a)

Control DLysCl DLysOD DLyshc

(b)

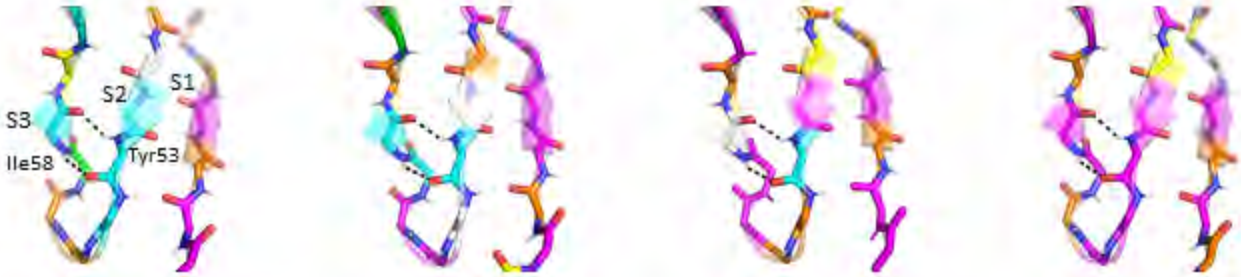

Control DLysCl DLysOD DLyshc

Figure 2

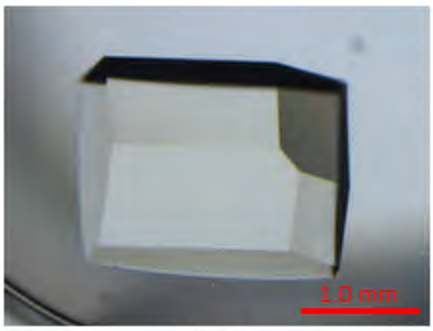

DLysCl

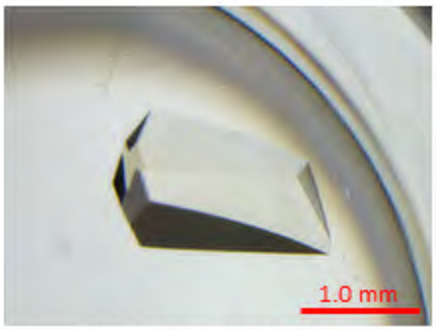

DLysOD

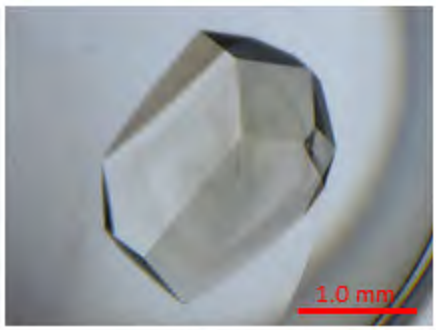

DLyshc

Figure S1.

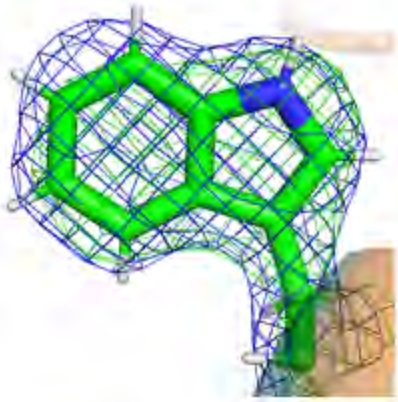

DLysCl

DLysOD

DLyshc

Figure S2.

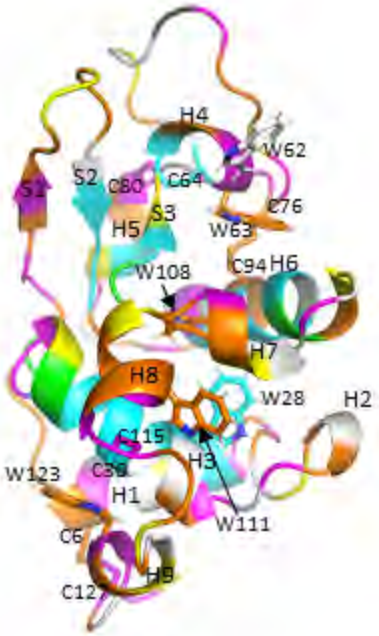

Cntl

DLysCl

DLysOD

DLyshc

Figure S3.